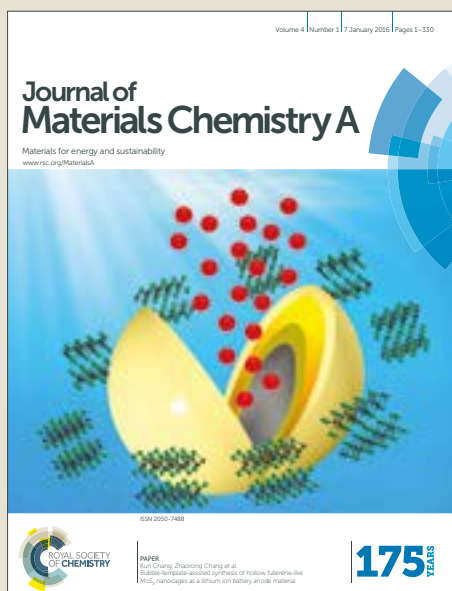


Journal of Materials Chemistry A

Accepted Manuscript



This article can be cited before page numbers have been issued, to do this please use: N. Kaur, S. Kaur, G. Kaur, A. Bhalla, S. S. Srinivasan and G. R. Chaudhary, *J. Mater. Chem. A*, 2019, DOI: 10.1039/C9TA05441C.



This is an Accepted Manuscript, which has been through the Royal Society of Chemistry peer review process and has been accepted for publication.

Accepted Manuscripts are published online shortly after acceptance, before technical editing, formatting and proof reading. Using this free service, authors can make their results available to the community, in citable form, before we publish the edited article. We will replace this Accepted Manuscript with the edited and formatted Advance Article as soon as it is available.

You can find more information about Accepted Manuscripts in the [author guidelines](#).

Please note that technical editing may introduce minor changes to the text and/or graphics, which may alter content. The journal's standard [Terms & Conditions](#) and the ethical guidelines, outlined in our [author and reviewer resource centre](#), still apply. In no event shall the Royal Society of Chemistry be held responsible for any errors or omissions in this Accepted Manuscript or any consequences arising from the use of any information it contains.

1 **Metallovesicles as smart nanoreactors for green catalytic synthesis of benzimidazole**
2 **derivatives in water**

3 Navneet Kaur,^a Simranpreet Kaur,^a Gurpreet Kaur,^a Aman Bhalla,^a Sessa Srinivasan^b and
4 Ganga Ram Chaudhary^{a*}

5 ^aDepartment of Chemistry & Centre for Advanced Studies in Chemistry, Panjab University,
6 Chandigarh-160014, India

7 ^bFlorida Polytechnic University, Lakeland-33805, Florida, USA

8
9

10
11
12
13
14
15
16
17
18
19
20
21
22
23
24
25
26
27
28
29
30
31
32
33
34
35
36
37
38
39
40

*Corresponding author.

Tel.: +91-172 2534406; Fax: +91-172-2545074

E-mail address: grc22@pu.ac.in (Ganga Ram Chaudhary)

41 **Abstract**

42 Metallovesicles are an emerging class of soft nanomaterials where spherical bilayer membranes,
43 resulting from self-aggregation of amphiphilic metal complexes, amalgamate the advantages of
44 metal specific catalytic properties and small hydrophobic cavities serving as nanoreactors. The
45 confinement of substrates in these vesicle bilayers, on account of hydrophobic interactions in
46 aqueous media, encourage their application in catalysis, particularly, where preclusion of organic
47 solvents is of prime concern without compromising desired reaction rates and product yields. In
48 the present work, novel amphiphilic metallosurfactant complex $[\text{Cu}(\text{C}_{12}\text{H}_{25}\text{NH}_2)_2]\text{Cl}_2$ has been
49 self-assembled to achieve spherical bilayer structures known as copper metallovesicles
50 (CuMVs). DLS, TEM and FESEM analyses revealed the formation of spherical multivesicular
51 vesicles in the size range 160-200 nm. The multivesicular structure of CuMVs was further
52 supported by small angle x-ray scattering (SAXS) results. The as-synthesized CuMVs were
53 further assessed for their potential as aqueous catalytic system for the synthesis of important
54 therapeutic agents, benzimidazoles. The co-existence of hydrophobic reactants inside the metal-
55 adorned vesicle bilayers, affords high product yield in short times. Facile synthesis of
56 metallosurfactants, self-assembly to metallovesicles, aqueous reaction media, low metal
57 concentration, low E-factor values, stability and recyclability of metallovesicles are the features
58 that establish metallovesicular catalysis as a promising multifaceted approach for greener
59 catalysis of benzimidazole synthesis and many other significant synthetic reactions.

60

61 **Keywords:** Metallovesicles, nanoreactor, metallosurfactant, benzimidazoles, green chemistry,
62 catalysis, water

63

64

65

66

67

68

69

70 1. Introduction

71 In recent years, the scientific community has become more sensitive towards environmental
72 issues and has worked illustriously in developing such protocols for synthesis of organic
73 molecules, which not only, are environment friendly but sustainable as well.¹ All the catalytic
74 approaches, whether they involve homogeneous or heterogeneous catalysts, are critically
75 examined on the scale of green chemistry.² Besides the cost and energy factor, the major factor
76 that decides the green nature of a catalytic protocol is the choice of reaction media.³ Many
77 organic syntheses that involve harmful organic solvents as reaction media are high on E-factor
78 value which is a prime concern in developing eco-friendly and sustainable protocols.⁴ Water, for
79 its inexpensive, non-toxic and non-flammable nature, has intrigued the scientists to develop
80 methods that favor organic syntheses of molecules in water.⁵ While heterogeneous catalysis in
81 water requires high temperatures (preferably microwaves), the homogeneous catalysis in
82 presence of water poses difficulties in separation of products and even contamination of water
83 for reuse.⁶ The challenge of combining the better selectivity of homogeneous catalysis with the
84 recoverability and reusability factor of heterogeneous catalysis puts forward the need of
85 developing innovative and smart materials that smartly address the demands of green catalysis.
86 Nanoreactors, comprising of the non-covalent self-assemblies of amphiphilic molecules, have
87 emerged as excellent alternatives to combine the features of homogeneous and heterogeneous
88 catalysis in one-pot.⁷ The amphiphilic nature of these self assemblies resolve the solubility issues
89 of substrates in water, which are held together in hydrophobic pockets of these self-assembled
90 nanoreactors. The compartmentalization of substrates results in their increased proximity and
91 concentration around active catalytic sites.⁸ In literature, a vast variety of amphiphilic aggregates
92 like micelles, vesicles, microemulsions, liposomes, polymerosomes etc. of suitable morphology
93 are known to enhance the reaction rates of many organic reactions.⁹⁻¹³ Vesicles, for instance,
94 have better catalytic performance in comparison to micelles and other aggregates¹⁴⁻¹⁶ because of
95 the following four factors¹⁷ (i) they possess chemical aspects of biological membranes and show
96 tremendous selectivity (ii) they increase the proximity between the reagents by decreasing the
97 effective volume where the reaction takes place (iii) their structural complexity provides
98 necessary steric-hindrance to avoid side reactions (iv) they provide reaction centers with
99 different polarity in comparison to the bulk solvent. Depending upon reaction requirements, the

100 fourth factor can be altered by incorporation of a metal ion into the vesicular structure. The
101 metallovesicles, formed as a result of functionalization of traditional vesicles with suitable metal
102 ions, are adorned with notable catalytic properties.¹⁸⁻¹⁹ Though there are numerous applications
103 of vesicular systems in drug delivery, model protocells, vaccination and reaction promoters²⁰⁻²⁴,
104 the metallovesicular systems are very less explored for their potential as efficient catalytic
105 systems.

106 The aim of the present work is two-fold; one, to fabricate metallovesicles (CuMVs) from
107 amphiphilic metallosurfactant complex, bisdodecylaminecopper(II)chloride and assess their
108 structural details. And two, to efficiently use the as-fabricated CuMVs, as catalyst, in synthesis
109 of benzimidazole derivatives in milder reaction conditions with water as solvent. Benzimidazole
110 and its derivatives are important building blocks of pharmaceutical industries owing to their
111 various biological activities such as antiarrhythmic,²⁵ antiulcer,²⁶ ionotropic,²⁷ antihelmintic,²⁸
112 anticancer²⁹ and antimicrobial activities.³⁰ Furthermore, these compounds have significant
113 industrial applications in UVB filters, optical devices, paints, and fuel cell membranes.³¹⁻³⁴ Many
114 reports are available in literature to synthesize benzimidazoles by the condensation of
115 arylaldehydes with ortho-phenylenediamines using variety of homogeneous and heterogeneous
116 catalysts, for e.g. acetic acid,³⁵ trimethylsilyl chloride,³⁶ oxone,³⁷ sulphamic acid,³⁸ $\text{PhI}(\text{OAc})_2$,³⁹
117 KHSO_4 ,⁴⁰ K_3PO_4 ,⁴¹ Amberlite,⁴² L-proline,⁴³ CoCl_2 ,⁴⁴ PTSA,⁴⁵ metal triflates,⁴⁶ heteropoly
118 acids,⁴⁷ solid support catalysts⁴⁸ and ionic liquids⁴⁹ etc. Unfortunately, many of these methods
119 suffer from drawbacks such as environmentally hazardous solvents/reagents, drastic reaction
120 conditions, low yields, tedious workup procedures, low atom economy and various side products.
121 Nanoparticles have also been utilized as heterogeneous catalysts in this synthesis but most of the
122 high-performing nanoparticles catalysts include expensive transition metals, hazardous oxidants
123 generating toxic by-products.⁵⁰⁻⁵⁶ As a consequence, the introduction of an efficient and mild
124 method is still needed to overcome these limitations. The present catalytic system, comprising of
125 CuMVs, offers a room temperature synthesis of 2-aryl-1*H*-benzimidazole derivatives at low
126 metal concentration in aqueous media which is economic, environmentally benign, recyclable
127 and energy efficient. The intriguing results obtained with CuMVs in the present synthetic
128 reaction with low E-factor values, expand their scope as catalysts in other reactions as well as
129 gives direction in designing similar catalytic structures with different functionalities.

130 2. Experimental

131 2.1. Materials

132 Copper(II) chloride (99%), dodecylamine (98.6%), o-phenylenediamine (99%), cholesterol
133 (99%) and DMSO-d₆ were purchased from Sigma Aldrich. Chloroform and diethyl ether were
134 purchased from Fischer Scientific. O-phenylenediamine (99%) was purchased from Sigma
135 Aldrich and various aromatic aldehydes (>98%) were purchased from Himedia. All the
136 chemicals were used as received without any further purification. Polycarbonate microfilters
137 (0.25 micron pore size) were purchased from Millipore.

138 2.2. Designing the catalyst

139 2.2.1. Fabrication of copper metallovessicles (CuMVs)

140 We are hereby proposing a catalyst design which adheres to all the prerequisites for the synthesis
141 of benzimidazole derivatives. In our previous report, we have described the synthesis of a
142 metallosurfactant complex, bisdodecylaminecopper(II) chloride [Cu(C₁₂H₂₅NH₂)₂]₂Cl₂⁵⁷ which is
143 used as precursor for the fabrication of CuMVs in present report.

144 The CuMVs were prepared by employing conventional chloroform film method.⁵⁸ Equimolar
145 amounts of [Cu(C₁₂H₂₅NH₂)₂]₂Cl₂ (5 mmol) and cholesterol (5 mmol) were dissolved in CHCl₃
146 (20 mL). The solution was stirred at 333 K in a round bottom flask for 30 minutes followed by
147 slow evaporation of CHCl₃ under reduced pressure. The resulting thin film on the surface of
148 round bottom flask was dried in vacuum desiccator at room temperature for 24 h and further
149 hydrated with deionized water (100 ml). The obtained solution was repeatedly sonicated,
150 subjected to vortex shaker for about 4 h and obtruded through polycarbonate microfilters (0.25
151 micron pore size) for at least 10 times which resulted in uniform particle size distribution as
152 monitored by Dynamic Light Scattering (DLS). Different volumes of this solution were further
153 used for catalytic synthesis of benzimidazole derivatives.

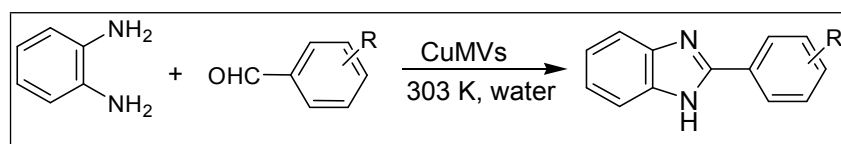
154 2.2.2. Characterization techniques

155 The formation of CuMVs was confirmed by different characterization techniques such as DLS,
156 Atomic Force Microscopy (AFM), Confocal Laser Scanning Microscopy (CLSM), Transmission
157 Electron Microscopy (TEM), Field Emission Scanning Electron Microscopy (FESEM) and
158 Small Angle X-ray Scattering (SAXS). Size measurements of CuMVs were done by DLS
159 experiments performed on ALV-5000 with Nd:YAG laser (wavelength 532 nm) at room

160 temperature. For TEM analysis, samples of CuMVs were dispersed on a carbon coated copper
161 grid and air dried grid was analyzed using Hitachi H 7500 instrument operated at 80-110 kV. For
162 FESEM images were taken with Hitachi (SU8010) at various operating voltages (3-20 kV). AFM
163 images were obtained on Nanoscope "V-multimode 8". The instrument was operated in the
164 contact mode with an operating frequency of 312.13 kHz. Confocal Laser Scanning Microscope
165 (CLSM) images were taken on Nikon Eclipse Ti(C2Si) inverted microscope (100x objective)
166 with attached Nikon camera. Nikon ECLIPSE E100 with attached camera was used to obtain
167 optical micrographs of CuMVs. SAXS studies were performed on SAXSpace by Anton Paar
168 operated on line collimation mode at 40 kV. Quartz capillary liquid cell of 1 mm diameter was
169 used to hold the sample. The scattering pattern was recorded using CCD detector having
170 scattering vector q ranges from 0.01 nm^{-1} to 8 nm^{-1} . All the measured intensity was normalised
171 and the background scattering contributions from capillary / solvent were corrected. The data
172 were evaluated with General Inverse Fourier Transformation (GIFT) software. The phase
173 transition temperature of metallosurfactant complex was found through Differential Scanning
174 Calorimetry (DSC), performed on DSC-Q20 (TA instrument, USA) at scanning range of 10° C
175 /min. ICP-MS analyses were done on ICP-MS Agilent 7800 to determine concentration of Cu in
176 metallovesicle solution.

177 2.3. Catalytic synthesis of 2-aryl-1*H*-benzimidazoles

178 **2.3.1. General procedure:** A mixture of *o*-phenylenediamine (1 mmol) and aromatic
179 aldehyde (1 mmol) was added to a round bottom flask containing CuMVs solution (20 ml,
180 containing 2 ppm Cu^{2+}) (scheme 1). The mixture was stirred well at 303 K, and the progress of
181 the reaction was monitored by thin layer chromatography at regular time intervals. As the
182 reaction proceeded to completion, the precipitation of product took place. After completion, the
183 reaction mixture was filtered to separate the product and obtained solid was recrystallized in
184 ethanol. Benzimidazole derivatives, which could not be crystallized, were purified with the help
185 of column chromatography.



186 **Scheme 1 Synthesis of 2-substituted benzimidazoles**

187 R = H, 2-OCH₃, 4-OCH₃, 4-NO₂, 3-NO₂, 4-Cl, 4-Br, 4-CN, 4-CH₃

188

189 **2.3.2. Characterization of products:** The identification of all the synthesized
190 benzimidazole derivatives was done through ^1H NMR using CDCl_3 as a solvent. The physical
191 and spectral data of all the products (Entries 1a-1i, Table 1) is given in supplementary
192 information (section S1, ESI).

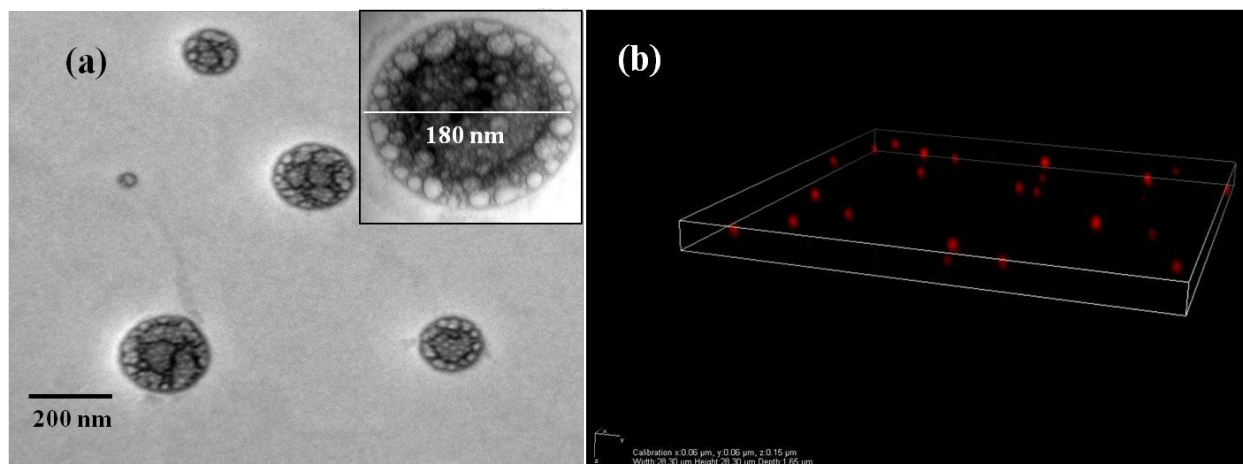
193 **2.3.3. Recycling the catalyst:** The CuMVs were collected as filtrate after filtration of
194 reaction mixture and were purified with diethyl ether to extract traces of unreacted substrates (if any).
195 The as-collected free aqueous CuMVs solution was used in next catalytic cycles to check their
196 recycling efficiency.

197 3. Results and Discussion

198 This article engulfs a green and highly efficient catalytic synthesis of benzimidazole derivatives
199 using specially designed aqueous CuMVs. Recyclable CuMVs have a dual role to play i.e. apart
200 from behaving as nano-vessels to accommodate reactants within them and increase their physical
201 proximity; they also provide acidic sites integrated within the aggregated structure that
202 expeditiously catalyzes the model reaction.

203 An amphiphilic metallosurfactant complex of copper equipped with two long
204 hydrocarbon chains *viz* $[\text{Cu}(\text{C}_{12}\text{H}_{25}\text{NH}_2)_2]\text{Cl}_2$ was synthesized and further used for the
205 preparation of CuMVs using film hydration method. The thin film as described in section 2.2.1
206 consists of sediments of multiple bilayers which were sonicated and mechanically vortexed with
207 deionised water at a temperature above the phase transition temperature (333 K) of
208 metallosurfactant complex (illustrated by DSC, Figure S1, ESI). This resulted in swelling and
209 folding of these lamellar bilayer structures into spherical CuMVs. The addition of equimolar
210 amounts of cholesterol to metallosurfactant complex was done to to meliorate rigidity and
211 stability of CuMVs.⁵⁹ The notably polydisperse CuMVs were repeatedly extruded (at least 10
212 times) through polycarbonate microfilters resulting in monodisperse CuMVs as monitored by
213 DLS.⁶⁰ DLS analyses of CuMVs before and after extrusion are given in (Figure S2, ESI)
214 respectively. The polydispersity index of CuMVs was reduced from 0.367 to 0.132 after
215 extrusion. The average size of extruded CuMVs was found to be 220 nm. It is to be noted that
216 amount of water used for hydration process has no effect on CuMVs' morphology. However, it
217 results in the variation of concentration of resulting CuMVs in solution.

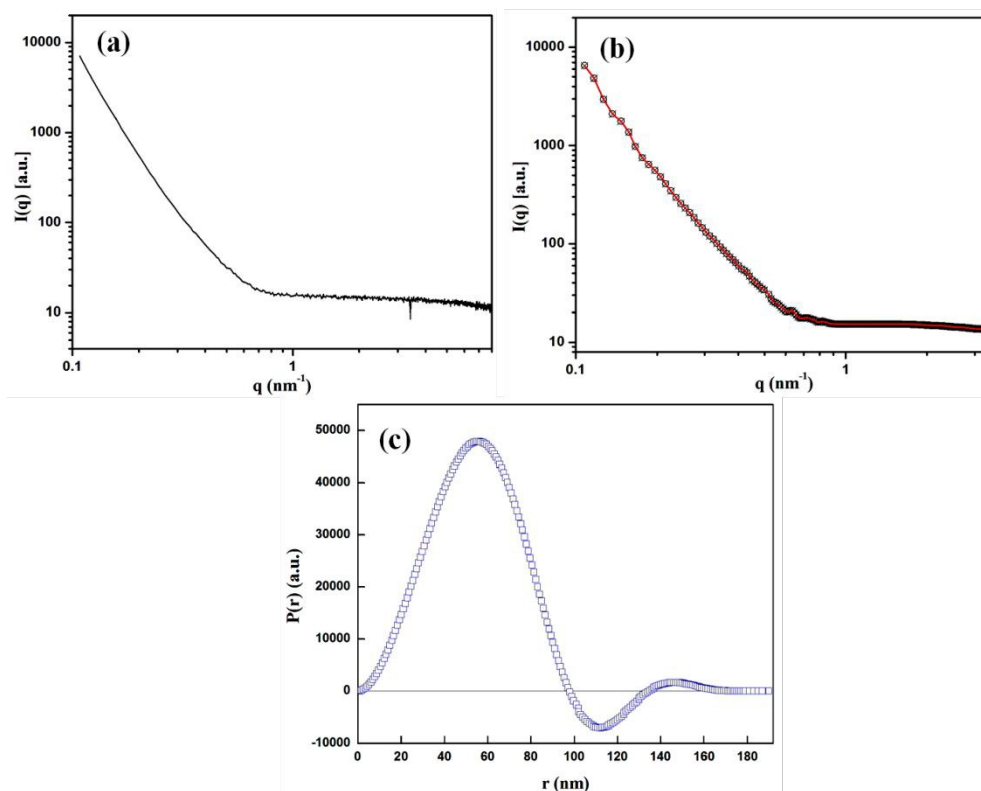
218 Morphological details of CuMVs were obtained by different microscopic techniques.
219 Preliminary structural examination of CuMVs was done with conventional light microscope that
220 showed spherical structures (Figure S3(a), ESI). Further detailed examination of size,
221 morphology and topography of the CuMVs was carried out using TEM, CLSM, FESEM and
222 AFM techniques. TEM, CLSM and FESEM analysis gave a fairer insight into the size,
223 morphology and lamellarity whereas AFM studies showed topographical analysis of the prepared
224 CuMVs. TEM image (Figure 1(a)) shows the formation of multivesicular metallovesicles (large
225 number of small vesicles inside a giant vesicle) in the size range 160-200 nm. Inset of Figure
226 1(a) shows high resolution TEM image of a multivesicular vesicle (180 nm). The spherical shape
227 of CuMVs is further confirmed through CLSM images (Figure 1(b)). Also, the FESEM results
228 affirm with those of TEM showing spherical shaped structures (Figure S3(b)).⁵⁸ AFM images
229 show height and phase topographies of CuMVs (Figure S3(c)⁵⁸ and S3(d), respectively). Color
230 contrast in height images reveals the average particle size of CuMVs in the range of 180-200 nm
231 however vesicles are found to be vertically compressed due to high local force applied by the tip
232 of the cantilever. Colour contrast in phase image shows distinct phase boundaries as we move
233 from one metallovesicle to other, showing segregated distribution of CuMVs. Careful analysis of
234 the phase images shows colour contrast within the same vesicle illustrating the presence of
235 different phases in accordance with multivesicular topography.



236
237 **Figure 1 Structural investigation of CuMVs showing (a) TEM micrograph, inset: single**
238 **multivesicular vesicle (b) CLSM image.**

239
240 Further structural investigation of CuMVs was done using SAXS. Figure 2(a) shows
241 experimental SAXS scattering profile of CuMVs in which scattering intensities $I(q)$ are plotted

242 as a function of scattering vector q , which is defined as $4\pi\sin\theta/\lambda$; where θ is half the scattering
 243 angle and λ is wavelength of X-rays. The absence of distinct diffraction maxima in SAXS profile
 244 suggested the lack of periodicity in the structures.⁶¹ This was indicative of multivesicular
 245 structure of CuMVs consisting of non-concentric bilayers. Also, the power law (q^{-1}) of scattering
 246 curve in line collimation mode suggested vesicular structures.⁶¹⁻⁶³ The interpretation of scattering
 247 curve in real space was done using General Inverse Fourier Transformation (GIFT) which
 248 generated Pair Distance Distribution Function (PDDF), $P(r)$. Figure 2(b) and (c) show the
 249 approximated SAXS scattering data fit with experimental data after carrying out indirect Fourier
 250 transformation and the corresponding PDDF, respectively. It can be seen that the data fits well
 251 with experimental data and the PDDF curve i.e. $P(r)$ v/s r shows asymmetry with alternate signs
 252 of distribution function. Since $P(r)$ is calculated by weighting two electron density values
 253 connected by distance r , the asymmetry in signs of $P(r)$ points towards inhomogenous interior of
 254 CuMVs.

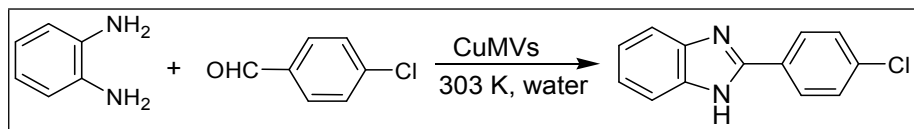


255
 256 **Figure 2(a) SAXS scattering profile of CuMVs (b) approximated scattering curve (red)**
 257 **after carrying out Indirect Fourier Transformation and (c) the corresponding PDDF.**

258
 259

260 3.1. Catalytic synthesis of 2-aryl-1H-benzimidazoles using CuMVs

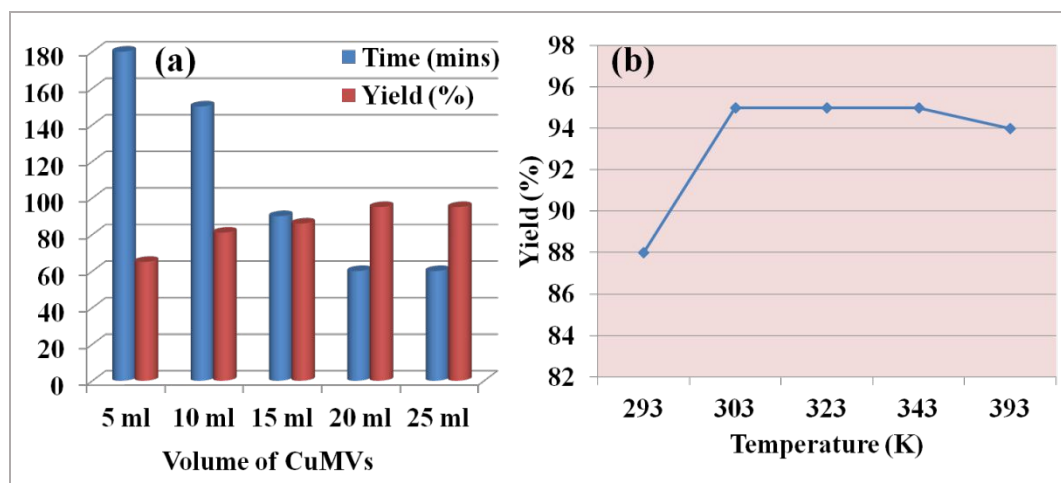
261 The CuMVs were tested for their catalytic efficiency in synthesis of various benzimidazole
 262 derivatives (Entries 1a-1i, Table 1). The optimum reaction conditions were obtained by choosing
 263 a model reaction between o-phenylenediamine and 4-chlorobenzaldehyde was chosen (scheme 2)
 264 to obtain the optimum reaction conditions by varying different reaction parameters like catalyst
 265 dose and temperature. In all the experiments, the progress of the reaction was monitored by thin
 266 layer chromatography and % product yield were noted.



267
268 Scheme 2 Model reaction between o-phenylenediamine and 4-chlorobenzaldehyde

269 Initially, a blank experiment was run where the model reaction was performed in the absence of
 270 CuMVs. The reaction did not show any progress even after 4 h suggesting the need of catalyst
 271 for successful conversion of reactants to product.

272 In order to optimize the catalyst dose for the reaction, the CuMVs solution was initially assessed
 273 for concentration of catalytically active sites (Cu^{2+}) using ICP-MS analysis that suggested it to be
 274 2 ppm. The model reaction was then carried out with different volumes of CuMVs solution.
 275 Figure 3(a) summarizes the time for reaction completion and isolated product yield in each case.
 276 An increase in the volume of CuMVs solution led to faster completion of reaction with increased
 277 product yield.



278
279 **Figure 3 (a) Effect of catalytic dose (b) variation of product yield with reaction temperature**

280 Reaction conditions (a): o-phenylenediamine (1 mmol), 4-chlorobenzaldehyde (1 mmol), CuMVs (2 ppm), 303 K (b) 20 ml.

281 * Isolated yield

282 The results could be understood in terms of increase in number of catalytically active Cu²⁺ sites.
283 Increasing the volume of solution ensured more number of CuMVs and hence faster reactions
284 with better yields. The constant results beyond 20 ml of catalyst volume suggest the complete
285 encapsulation of reactants in the CuMVs. Introduction of anymore amount of CuMVs did not
286 affect the reaction rate as there was no further encapsulation of reactants in newly introduced
287 CuMVs. The catalytic reaction was also performed at higher temperatures to understand the
288 effect of temperature on the reaction performance. It was found that increasing the reaction
289 temperature had negligible effect on product yield (Figure 3(b)). Based on these results, the
290 optimum reaction temperature for the reaction was fixed to be 303 K.

291 3.2. Substrate scope

292 The designed catalytic system has wide applicability as it covers a large number of substrates
293 for the synthesis of various benzimidazole derivatives. The reaction was performed with
294 different aromatic aldehydes carrying different substituents and good to excellent product yields
295 were obtained in all the cases (Table 1). The reaction times are greatly influenced by the electron
296 releasing or withdrawing nature of substituents attached to the aromatic ring. As expected from
297 the first step of mechanism which is nucleophilic attack of o-phenylenediamine on aromatic
298 aldehyde, electron withdrawing groups increase the electrophilicity of carbonyl carbon favouring
299 the nucleophilic attack. This accounts for the lower reaction times for electron withdrawing
300 groups as compared to electron releasing groups. However, for same group longer reaction times
301 were observed for the ortho and meta substitutions due to steric reasons.

302 3.3. E-factor calculations

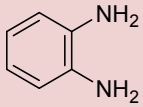
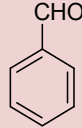
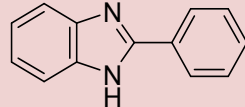
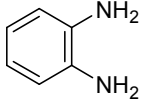
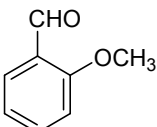
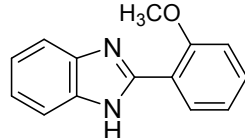
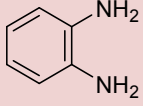
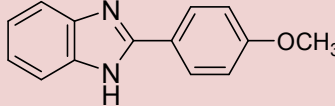
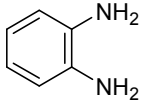
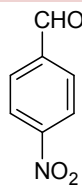
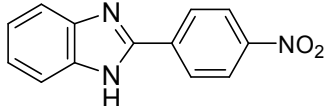
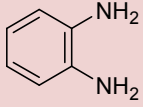
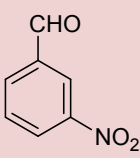
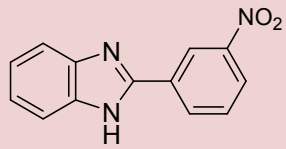
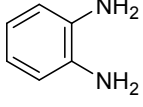
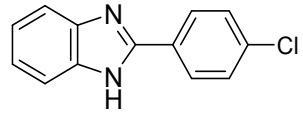
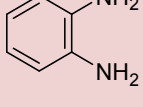
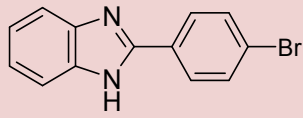
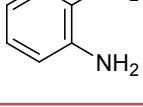
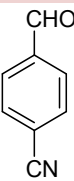
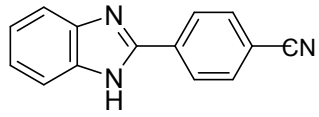
303 The environmental impact of the catalytic protocol was assessed through E-factor calculations
304 which measures the amount of waste generated during a synthetic process. The calculations were
305 done using Eq. 1 as follows:

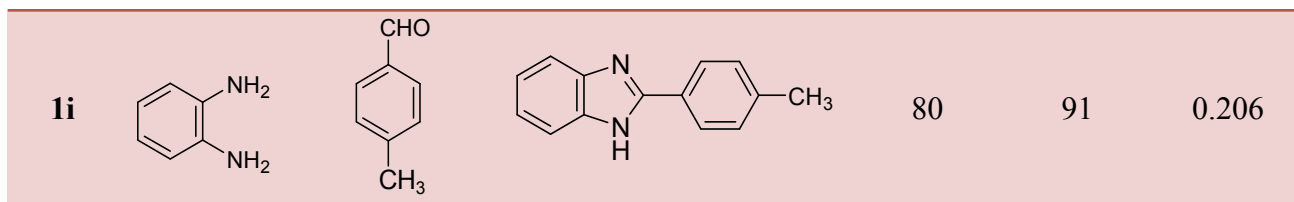
$$306 \quad \text{E-factor} = \frac{\text{Mass of waste generated during the reaction (in g)}}{\text{Mass of the desired product formed (in g)}} \quad \text{Eq. 1}$$

307 It is to be noted that since the CuMVs were recovered during the process for further usage, mass
308 of CuMVs have been omitted from the E-factor calculations. The values of E-factor have been
309 calculated for synthesis of all the benzimidazole derivatives and are given in Table 1. It can be
310 seen from Table 1 that E-factor values are very small ranging between 0.14 and 0.21 which
311 advocates the green nature of the protocol. This is attributed to minimum waste generation

312 during the process which occurs in water as reaction medium in presence of highly active
313 recyclable CuMVs.

314 **Table 1** Effect of substituent (on aromatic aldehyde) on reaction rate

Entry	Diamine	Aromatic aldehyde	Product	Time (mins)	Yield (%) [*]	E-factor
1a				70	94	0.175
1b				85	90	0.212
1c				80	93	0.173
1d				45	95	0.142
1e				50	93	0.166
1f				60	95	0.148
1g				75	95	0.130
1h				60	96	0.138

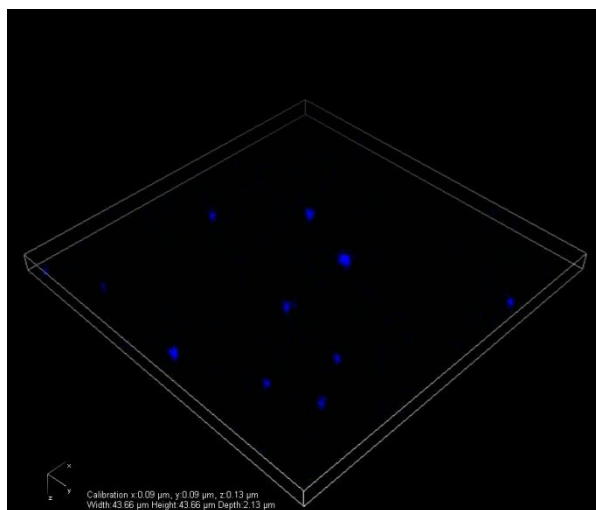


315 Reaction conditions: o-phenylenediamine (1 mmol), aromatic aldehyde (1 mmol), CuMVs (2 ppm, 20 ml), 303 K

316 * Isolated yield

317 3.4. Mechanistic aspects of catalysis with CuMVs

318 The CuMVs act as small nanoreactors bearing catalytically active Cu^{2+} sites. The hydrophobic
319 pockets inside the multivesicular structure of CuMVs encapsulate the substrates and increase
320 their concentration at catalytically active Cu^{2+} sites resulting in faster catalysis. This
321 encapsulation of substrates in hydrophobic regions is evidenced through CLSM image of
322 CuMVs encapsulated with reactant (4-bromobenzaldehyde) (Figure 4).



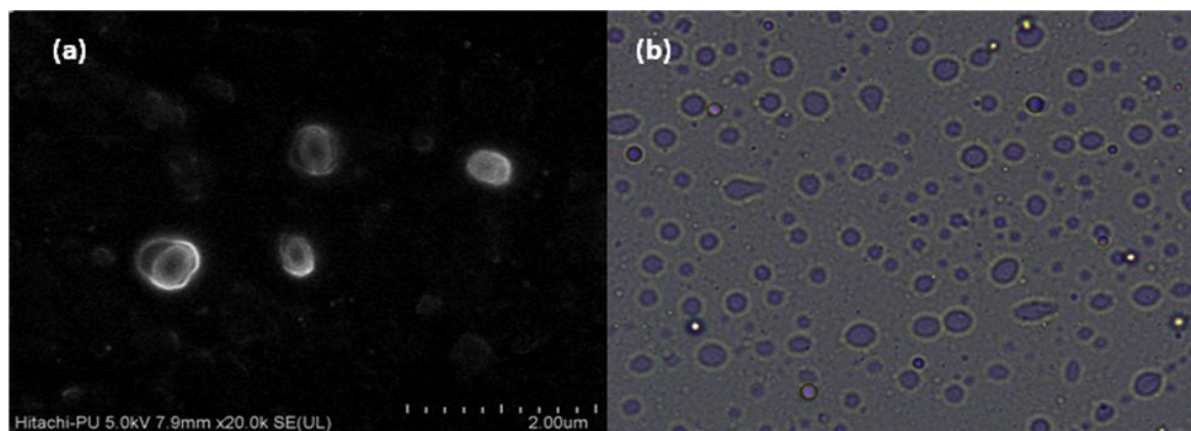
323
324 **Figure 4 CLSM micrograph of CuMVs loaded with 4-bromobenzaldehyde.**

325 The proposed mechanism for the reaction taking place inside the CuMVs is depicted in Scheme
326 S1 (ESI). The Cu^{2+} sites in the CuMVs activate the carbonyl carbon of the aromatic aldehyde for
327 nucleophilic attack by $-\text{NH}_2$ group of o-phenylenediamine. The resulting imine is further
328 attacked by second $-\text{NH}_2$ to form dihydroimidazole followed by aromatization in presence of air
329 to give 2-aryl-1*H*-benzimidazoles as product.

330

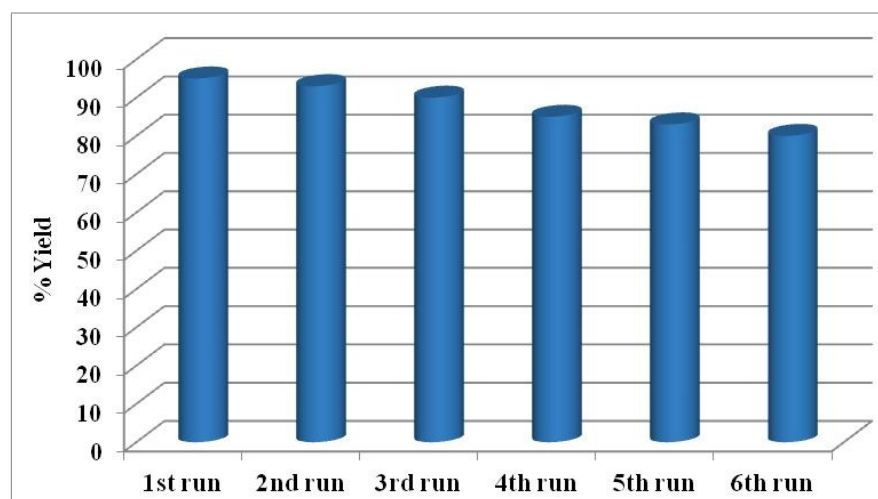
331 3.5. Reusability Tests

332 The developed catalytic system was assessed for its recycling efficiency. Firstly, the CuMVs
333 solution recycled after 1st reaction cycle was investigated for structural integrity of CuMVs
334 using FESEM and Light microscope (Figure 5). It can be seen from FESEM image (Figure 4(a))
335 and optical micrographs (Figure 5(b)) that the recycled CuMVs maintained their structural
336 integrity.



337
338 **Figure 5 (a) FESEM image and (b) optical micrograph of CuMVs recovered after 1st cycle**
339 **of catalytic reaction.**

340 The recycled CuMVs solution was subjected to further catalytic cycles and the reaction
341 performance was noted in each case. It was found that the CuMVs maintained their catalytic
342 performance for up to 6 reaction cycles (Figure 6). The performance is attributed to mechanical
343 strength and stability of metallovesicular structures.



344
345 **Figure 6 Recycling efficiency of CuMVs**

346 The decline in the performance of the catalytic system can be explained on the basis of rupture of
347 metallovesicle structure on repeated use beyond 6th cycle (Figure S4, ESI).

348 4. Advantage over other catalytic systems and future prospects

349 The synthesis of 2-aryl-1*H*-benzimidazole derivatives has been achieved with a number of
350 catalysts in literature. The reaction conditions and their catalytic performance are tabulated in
351 Table 2. It can be seen that most of the catalysts, apart from their own toxic nature, require high
352 temperatures, toxic solvents as reaction medium and tedious work-up procedures to separate the
353 products. The transition metal oxide nanoparticles (In₂O₃),⁵⁰ though prove to be an efficient
354 alternative in terms of their activity and recoverability, compromise with the cost factor which
355 cannot be ignored for the implementation of the protocol on large scale. The present system is
356 found to qualify all the significant conditions of an efficient catalytic system like high activity,
357 environment benignity, cost effectiveness, recyclability and ease of product separation. The
358 catalytic systems consisting of metallovesicles have a promising scope in future of metal-assisted
359 catalysis of organic reactions and transformations which, otherwise, require traditional organic
360 solvents and expensive metal catalysts.

361 **Table 2** Comparison of catalytic performance of present catalytic system with literature reports
362 for the synthesis of 2-substituted benzimidazoles.

S. No.	Catalyst	Catalyst dose	Time/ yield (%)	Solvent/ Temperature	Ref.
1.	VOSO ₄	3 mol %	1 h/ 92 %	EtOH/ rt	[64]
2.	TiCl ₃ OTf	10 mol %	50 mins/ 86 %	EtOH/ rt	[65]
3.	Ce(NO ₃) ₃ .6H ₂ O	30 mol %	1.5-2 h/93 %	DMF/ 80°C	[66]
4.	PhSiH ₃	4 equivalent	2 h/ 95 %	DMF/120°C	[67]
5.	Co(OH) ₂	10 mol %	4-7 h/ 82-96 %	EtOH/ rt	[68]
6.	ClSO ₃ H	10 mol %	1.8 h/ 93 %	2-propanol/ rt	[69]

7.	CuFe ₂ O ₄ NPs	20 mol%	24 h/89%	toluene/O ₂	[51]
8.	Mesoporous TiO ₂ -Fe ₂ O ₃	20 mg	3h/97%	H ₂ O/O ₂	[52]
9.	Pt/TiO ₂	1 mol%	1h/78%	mesitylene	[53]
10.	Fe ₃ O ₄ -SiO ₂ - (NH ₄) ₆ Mo ₇ O ₂₄ nanocomposite	220 mg	0.5 h/90%	EtOH/H ₂ O ₂	[54]
11.	α-MoO ₃ nanobelts	2 mol%	0.5 h/93%	t-BuOOH	[55]
12.	CuI Nps	10 mol%	1 h/96%	CH ₃ CN/O ₂	[56]
13.	CuMVs	0.03 mol%	1 h/96%	H ₂ O	Present work

363

364

365

5. Conclusions and Outlook

366 In conclusion, novel metallovesicles, CuMVs have been fabricated using metallosurfactant
 367 complex, bisdodecylaminecopper(II)chloride. The as-fabricated metallovesicles have been
 368 employed as nanoreactors for the catalytic synthesis of 2-aryl-1*H*-benzimidazole. The successful
 369 condensation of *o*-phenylenediamine with aromatic aldehydes in aqueous metallovesicles
 370 solutions under mild reaction conditions to give excellent product yields, establish the claim of
 371 these novel metallovesicles as small nanoreactors possessing active catalytic sites. The notable
 372 catalytic activity, harmless aqueous reaction medium, ambient reaction conditions promote the
 373 as-developed catalytic approach as effective and greener approach for benzimidazole synthesis.
 374 The strength and stability of metallovesicular structures impart yet another attractive feature to
 375 the catalytic approach in the form of recyclability. Effective catalytic action followed by facile
 376 recovery of metallovesicles enables them to be reused in further reaction cycles. The efficiency
 377 of CuMVs as catalysts in the present protocol opens up the way to diverse applications of these
 378 materials in the field of organic synthesis which requires a dire need to shift to efficient, greener
 379 and sustainable catalytic approaches.

380

381 Conflicts of interest

382 Authors declare no conflicts of interest.

383 Acknowledgements

384 Ganga Ram Chaudhary and Sesha Srinivasan would like to acknowledge the support of UGC,
385 India under INDO-US 21st Century Knowledge Initiative project [F.No. 194-2/2016 (IC)].
386 Navneet Kaur is thankful to UGC for Senior Research Fellowship. Gurpreet Kaur acknowledges
387 DST, India for Inspire Faculty award (IFA-12-CH-41). All the authors acknowledge the support
388 of DST PURSE II grant for this work.

389 References

- 390 [1] Liu, Y.; Wang, W.; Xu, X.; Veder, J. P.; Shao, Z. *J. Mater. Chem. A*. 2019
391 <http://dx.doi.org/10.1039/C8TA09913H>
- 392 [2] Mulvihill, M. J.; Beach, E. S.; Zimmerman, J. B.; Anastas, P. T. *Annu. Rev. Environ.*
393 *Resour.* 2011, **36**, 271-293.
- 394 [3] Polshettiwar V.; Varma R. S. *Acc. Chem. Res.* 2008, **41(5)**, 629-639.
- 395 [4] Kaur, N.; Kaur, G.; Bhalla, A.; Dhau, J.; Chaudhary, G. R. *Green Chem.* 2018, **20**, 1506-
396 1518.
- 397 [5] Gawande, M. B.; Bonifácio, V. D.; Luque, R.; Branco, P. S.; Varma, R.S. *Chem. Soc.*
398 *Rev.* 2013, **42(12)**, 5522-5551.
- 399 [6] Dekker, F. H. M.; Blik, A.; Kapteijn, F.; Moulijn, J. A. *Chem. Eng. Sci.* 1995, **50**, 3573-
400 3580.
- 401 [7] De Martino, M. T.; Abdelmohsen, L. K.; Rutjes, F. P.; van Hest, J. C. *Beilstein J. Org.*
402 *Chem.* 2018, **14(1)**, 716-733.
- 403 [8] Leenders, S. H. A. M.; Gramage-Doria, R.; de Bruin, B.; Reek, J. N. H. *Chem. Soc. Rev.*
404 2015, **44**, 433-448.
- 405 [9] Dwars, T.; Paetzold, E.; Oehme, G. *Angew. Chem. Int. Ed.* 2005, **44**, 7174-7199.
- 406 [10] Tonova, K.; Lazarova, Z. *Biotechnol. Adv.* 2008, **26(6)**, 516-532.
- 407 [11] Akbarzadeh, M.; Moosavi-Movahedi, Z.; Shockravi, A.; Jafari, R.; Nazari, K.; Sheibani,
408 N.; Moosavi-Movahedi, A. A. *J. Mol. Catal. A: Chem.* 2016, **424**, 181-193.

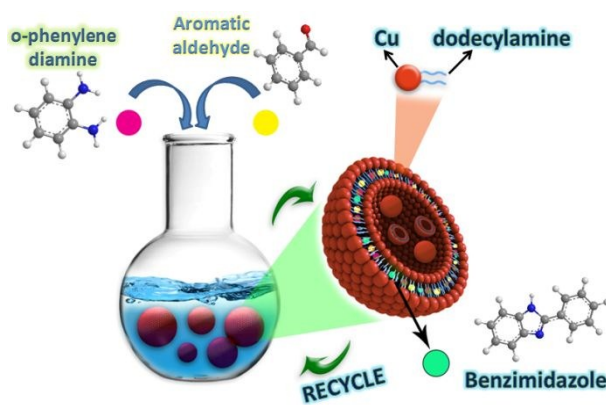
- 409 [12] Jiang, Y.; Wang, D.; Pan, Z.; Ma, H.; Li, M.; Li, J.; Zheng, A.; Lv, G.; Tian, Z. *Front.*
410 *Chem. Sci. Eng.* 2018, **12(1)**, 32-42.
- 411 [13] Hirose, M.; Ishigami, T.; Suga, K.; Umakoshi, H. *Langmuir* 2015, **31(47)**, 12968-12974.
- 412 [14] Kunitake, T.; Okabata, Y.; Ando, R.; Shinkai, S.; Hirakawa, S. *J. Am. Chem. Soc.* 1980,
413 **102**, 7877-7881.
- 414 [15] Scarpa, M.V.; Araujo, P. S.; Schreier, S.; Sesso, A.; Oliveira, A. G.; Chaimovich, H.;
415 Cuccovia, I. M. *Langmuir* 2000, **16**, 993-999.
- 416 [16] Perez-Juste, J.; Hollfelder, F.; Kirby, A. J.; Engberts, J.B.F.N. *Org. Lett.* 2000, **2**, 127-
417 130.
- 418 [17] Walde, P.; Umakoshi, H.; Stano, P.; Mavelli, F. *Chem. Commun.* 2014, **50**, 10177-
419 10197.
- 420 [18] Rispens, T.; Engberts, J.B.F.N. *Org. Lett.* 2001, **3**, 941-943.
- 421 [19] Gruber, B.; Kataev, E.; Aschenbrenner, J.; Stadlbauer, S.; König, B. *J. Am. Chem. Soc.*
422 2011, **133(51)**, 20704-20707.
- 423 [20] Szostak, J. W.; Bartel, D. P.; Luisi, P. L. *Nature* 2001, **409**, 387-390.
- 424 [21] Noireaux, V.; Libchaber, A. *Proc. Natl. Acad. Sci. U. S. A.* 2004, **101**, 17669-17674.
- 425 [22] Walde, P. *Bioessays* 2010, **32**, 296-303.
- 426 [23] Stano, P.; Carrara, P.; Kuruma, Y.; de Souza, T. P.; Luisi, P. L. *J. Mater. Chem.* 2011,
427 **21**, 18887-18902.
- 428 [24] Matosevic, S. *Bioessays* 2012, **34**, 992-1001.
- 429 [25] Horton, D. A.; Bourne, G. T.; Smythe, M. L. *Chem. Rev.* 2003, **103**, 893-930.
- 430 [26] Undevia, S. D.; Innocenti, F.; Ramirez, J.; House, L.; Desai, A. A.; Skoog, L. A.; Singh,
431 D. A.; Karrison, T.; Kindler, H. L.; Ratain, M. J. *Eur. J. Cancer* 2008, **44**, 1684-1692.
- 432 [27] Lixin, Z.; Arnold, L. D.; Natural Products: Drug Discovery and Therapeutic Medicine;
433 Humana Press: Totowa, NJ, 2005, 341.
- 434 [28] Jakubke, H. D.; Sewald, N. Peptides from A to Z: A Concise Encyclopedia;
435 Wiley-VCH Verlag GmbH & Co. KGaA: Weinheim, Germany, 2008, 378.
- 436 [29] Mehlhorn, H., Ed. Encyclopedia of Parasitology, Vol. 3; Springer-Verlag: Berlin, 2008,
437 386.

- 438 [30] Sarges, R.; Howard, H. R.; Browne, R.G.; Lebel, L. A.; Seymour, P. A.; Koe, B. K. *J.*
439 *Med. Chem.* 1990, **33**, 2240-2254.
- 440 [31] Fritsch, P. In *Dermatologie und Venerologie*, Vol. 2; Springer-Verlag: Berlin, 2004.
- 441 [32] Smith, H. M. *High Performance Pigments*; Wiley-VCH Verlag GmbH & Co. KGaA:
442 Weinheim, Germany, 2002, 135-158.
- 443 [33] Meuthen, B.; Jandel, A. S. *Coil Coating*, 2. Auflage, Friedr. Vieweg & Sohn Verlag:
444 Wiesbaden, Germany, 2008, 65.
- 445 [34] Scherer, G. G. *Fuel Cells II*; Springer-Verlag: Berlin, 2008, 65-120.
- 446 [35] Azarifari, D.; Pirhayati, M.; Maleki, B.; Sanginabadi, M.; Yami, R. N. *J. Serb. Chem.*
447 *Soc.* 2010, **75**, 1181-1189.
- 448 [36] Wan, J. P.; Gan, S. F.; Wu, J. M.; Pan, Y. *Green Chem.* 2009, **11**, 1633-1637.
- 449 [37] Beaulieu, P. L.; Hache, B.; Moon, V. E. *Synthesis* 2003, **11**, 1683-1692.
- 450 [38] Chakrabarty, M.; Karmakar, S.; Mukherji, A.; Arima, S.; Harigaya, Y. *Heterocycles*
451 2006, **16**, 4169-4173.
- 452 [39] Du, L. H.; Wang, Y. G. *Synthesis* 2007, **5**, 675-678.
- 453 [40] Ma, H.; Wang, Y.; Wang, A. *Heterocycles* 2006, **68**, 1669-1673.
- 454 [41] Xie, C., Han, X.; Gong, J.; Li, D.; Ma, C. *Org. & Biomol. Chem.* 2017, **15**, 5811-5819.
- 455 [42] Sharma, S. D.; Konwar, D. *Synth. Commun.* 2009, **39**, 980-991.
- 456 [43] Varala, R.; Nasreen, A.; Enugala, R.; Adapa, S. R. *Tetrahedron Lett.* 2007, **48**, 69-72.
- 457 [44] Khan, A. T.; Parvin, T.; Choudhury, L. H. *Synth. Commun.* 2009, **39**, 2339-2346.
- 458 [45] Han, X.; Ma, H.; Wang, Y.; *Arkivoc* 2007, **13**, 150-154.
- 459 [46] (a) Torabi, P.; Azizian, J.; Noei, J. *Tetrahedron Lett.* 2016, **57**, 185-188.
460 (b) Itoh, T.; Nagata, K.; Ishikawa, H.; Ohsawa, A. *Heterocycles* 2004, **63**, 2769-2783.
461 (c) Trivedi, R.; De, S. K.; Gibbs, R. A. *J. Mol. Catal. A: Chem.* 2005, **245**, 8-11.
- 462 [47] Heravi, M. M.; Sadjadi, S.; Oskooie, H. A.; Shoar, R. H.; Bamoharram, F. F. *Catal*
463 *Commun.* 2008, **8**, 504-507
- 464 [48] Ben-Alloum, A.; Bakkas, S.; Soufiaoui, M. *Tetrahedron Lett.* 1998, **39**, 4481-4484.
- 465 [49] Ma, H. Q.; Wang, Y. L.; Li, J. P.; Wang, J. Y. *Heterocycles* 2007, **71**, 135-140.
- 466 [50] Santra, S.; Majee, A.; Hajra, A. *Tetrahedron Lett.* 2012, **53**, 1974-1977.

- 467 [51] Yang, D.; Zhu, X.; Wei, W.; Sun, N.; Yuan, L.; Jiang, M.; You, J.; Wang, H. *RSC Adv.*
468 2014, **4**, 17832-17839.
- 469 [52] Roy, S.; Banerjee, B.; Salam, N.; Bhaumik, A.; Islam, S. M. *ChemCatChem* 2015, **7**,
470 2689-2697.
- 471 [53] Chaudhari, C.; Hakim Siddiki, S. M. A.; Shimizu, K. *Tetrahedron Lett.* 2015, **56**, 4885-
472 4888.
- 473 [54] Bai, G.; Lan, X.; Liu, X.; Liu, C.; Shi, L.; Chen, Q.; Chen, G. *Green Chem.* 2014, **16**,
474 3160-3168.
- 475 [55] Jafarpour, M.; Rezaeifard, A.; Ghahramaninezhad, M.; Tabibi, T. *New J. Chem.* 2013,
476 **37**, 2087-2095.
- 477 [56] Linga Reddy, P.; Arundhati, R.; Tripathi, M.; Rawat, D. S. *RSC Adv.* 2016, **6**, 53596-
478 53601.
- 479 [57] Kaur, G.; Singh, P.; Mehta, S. K.; Kumar, S.; Dilbaghi, N.; Chaudhary, G. R. *Appl. Surf.*
480 *Sci.*, 2017, **404**, 254-262.
- 481 [58] Kaur, B.; Kaur, G.; Chaudhary, G. R. *J. Mater. Chem. B* 2019 DOI:
482 10.1039/C9TB00607A.
- 483 [59] Orathai, P.; Chavadej, S.; Rujiravanit, R. *J. Biosci. Bioeng.* 2011, **112**, 102-106.
- 484 [60] Hongwei, Z. *Liposomes*. Humana Press, New York, NY, 2017. 17-22.
- 485 [61] Moghaddam, M. J.; de Campo, L.; Hirabayashi, M.; Bean, P. A.; Waddington, L. J.;
486 Scoble, J. A.; Coiac, G.; Drummond, C. J. *Biomater. Sci.* 2014, **2**, 924-935.
- 487 [62] Malinda Salim, M.; Iskandar, W. F. N. W.; Patrick, M.; Zahid, N. I.; Hashim, R.
488 *Langmuir* 2016, **32**, 5552-5561
- 489 [63] Anton Paar GmbH.SAXS-Data Classification 01-Basics.
490 [http://www.msg.ucsf.edu/XRayLab/SAXS-Lit/SAXS-](http://www.msg.ucsf.edu/XRayLab/SAXS-Lit/SAXS-Data%20Classification%20%26%20Evaluation.pdf)
491 [Data%20Classification%20%26%20Evaluation.pdf](http://www.msg.ucsf.edu/XRayLab/SAXS-Lit/SAXS-Data%20Classification%20%26%20Evaluation.pdf).
- 492 [64] Digwal, C. S.; Yadav, U.; Sakla, A. P.; Ramya, P. V. S.; Aaghaz, S.; Kamal, A.
493 *Tetrahedron Lett.* 57, 2016, 4012-4016.
- 494 [65] Azizian, J.; Torabi, P.; Noei, J. *Tetrahedron Lett.* 2016, **57**, 185.
- 495 [66] Martins, G. M.; Puccinelli, T.; Gariani, R. A.; Xavier, F. R.; Silveira, C. C.; Mendes, S.
496 R. *Tetrahedron Lett.* 2017, **58**, 1969-1972.

- 497 [67] Zhu, J.; Zhang, Z.; Miao, C.; Liu, W.; Sun, W. *Tetrahedron* 2017, **73**, 3458-3462.
- 498 [68] Chari, M. A.; Shobha, D.; Sasaki, T. *Tetrahedron Lett.* 2011, **52**, 5575-5580.
- 499 [69] Shitole, N. V.; Niralwad, K. S.; Shingate, B. B.; Shingare, M. S. *Arab. J. Chem.* 2016, **9**,
- 500 S858- S860.

Graphical Abstract



Green catalytic synthesis of benzimidazoles using Cu metallovessicles as nanoreactors